

Stability of $4f$ configurations in rare-earth-metal compounds

C. Laubschat, G. Kaindl, and W.-D. Schneider*

Institut für Atom- und Festkörperphysik, Freie Universität Berlin, D-1000 Berlin 33, Germany

B. Reihl

IBM Zürich Research Laboratory, CH-8803 Rüschlikon, Switzerland

N. Mårtensson

Institute of Physics, Box 530, S-75121, Uppsala, Sweden

(Received 18 September 1985)

Surface effects of the $4f$ and $5p$ binding energies as well as on the valence state were investigated for the dialuminides of the heavy rare-earth (RE) metals by high-resolution photoemission (PE) spectroscopy using synchrotron radiation. For comparison, Eu, Yb, and Lu metals as well as YbZn_2 were also studied. Complementary bremsstrahlung isochromat spectroscopy measurements were performed on GdAl_2 , ErAl_2 , and TmAl_2 . A pronounced difference in the magnitude of the surface core-level shifts and the intensity of the surface signals was observed between trivalent and divalent (including mixed-valent) RE compounds. The considerably larger shifts of the divalent (mixed-valent) compounds as compared to the trivalent ones are shown to be due to the larger heat of compound formation for the latter. The high surface-to-bulk intensity ratio in the PE spectra of divalent and mixed-valent compounds is discussed alternatively in terms of either a reduced mean free path due to the $4f$ scattering or a possible surface segregation of RE ions. On the basis of Johansson's stability diagram for RE metals and the measured $4f$ binding energies for compounds, a simple scheme is presented which allows a prediction of $4f$ configurational stability in a whole series of RE compounds. In agreement with this model, a divalent surface layer was observed for trivalent SmAl_2 , but not for SmPd_3 .

I. INTRODUCTION

The study of solid surfaces has attracted increasing interest in the last few years, since a number of interesting phenomena are connected with the loss of symmetry and the related change in coordination of atoms at the surface: surface core-level binding-energy shifts,¹ surface relaxations and reconstructions,² as well as surface valence transitions.³ From the experimental point of view, high-resolution photoemission (PE) techniques play an important role in the investigation of these phenomena, since the small mean free path of the photoelectrons renders these methods particularly surface sensitive, allowing a direct insight into changes of the electronic structure in the surface region of a solid.

The rare-earth (RE) metals are particularly well suited for such surface-oriented studies since the localized $4f$ electrons lead to sharp final-state multiplet structures in the PE spectra, so that surface effects may be investigated with high resolution. Moreover, the competition between $4f$ promotional energy and cohesive energy can lead to definite valence changes (in terms of the $4f$ occupation number) and therefore to qualitative changes in the chemical and physical properties of the solid surface.⁴

In the present work we report on a systematic PE study of the RE dialuminides in the photon-energy range $20 \leq h\nu \leq 110$ eV. For GdAl_2 , ErAl_2 , and TmAl_2 , complementary bremsstrahlung-isochromat-spectroscopy (BIS) measurements were performed. These intermetallic com-

pounds crystallize in the cubic MgCu_2 Laves phase; with the exception of Eu and Yb, all RE ions are trivalent in these intermetallics. Eu is divalent in EuAl_2 ,⁵ while Yb exhibits a mixed-valent behavior in YbAl_2 .⁶ In order to include a similar but completely divalent Yb compound, we extended the systematics to YbZn_2 ;⁷ we also compared the experimental results with those for the elemental RE metals and other RE compounds. On the basis of experimentally determined binding-energy shifts for the $4f$ and $5p$ core levels, we observe a linear relationship between the surface and the bulk shifts as well as a distinctly different behavior of divalent and trivalent RE systems. This behavior can be described in a quantitative way by relating the shifts to formation energies for the RE compounds in different valence states.^{4,8} For the heats of formation, we use the semiempirical model of Miedema.^{9,10} Moreover, we are able to correlate the magnitude of the core-level shifts with the occurrence of a surface valence transition in SmAl_2 , and establish a simple scheme for the $4f$ configurational stability of several series of RE compounds. The observed high surface-to-bulk emission ratio for the divalent and mixed-valent RE compounds is alternatively discussed in terms of surface segregation versus changes in the electron mean free path.

II. EXPERIMENTAL DETAILS

The room-temperature PE experiments were performed at the Synchrotron Radiation Center of the University of

Wisconsin—Madison, using a display-type photoelectron spectrometer and a toroidal-grating monochromator for photon energies $20 \leq h\nu \leq 110$ eV.¹¹ Electrons were accepted within an 86° cone with axis normal to the surface. The overall resolution of the system was 0.17 eV [full width at half maximum (FWHM)] at $h\nu=70$ eV. All samples were studied in polycrystalline form, with the exception of EuAl_2 , which was available as a single crystal. The Laves-phase compounds were fractured *in situ* and studied within 10–120 min after fracturing. No changes of the spectral features were observed within this period in a vacuum of 4×10^{-11} Torr. The samples of Eu and Yb metal were evaporated *in situ* on stainless-steel substrates, and the Lu surface was cleaned by scraping with a diamond file. The BIS experiments were performed at $h\nu=1486$ eV with a modified Vacuum Generators ESCA-III photoelectron spectrometer, equipped with a specially designed electron gun, a Johann-type x-ray monochromator, and a photon detector.¹² The total-system resolution was about 0.7 eV (FWHM). In the BIS measurements the samples were filed *in situ* every 4 min in a vacuum of 8×10^{-10} Torr in order to avoid oxygen contamination.

In all RE systems studied in this work, the given assignment of spectral features in the PE spectra as bulk or surface emission spectra is based on the observed photon-energy dependence of the valence-band spectra, which—in all cases—is characterized by a strong decrease of the surface $4f$ emission with increasing photon energy. This photon-energy dependence is expected from the known energy dependence of the electron mean free path in other RE systems.¹³

The PE spectra could be least-squares-fitted to a superposition of surface-derived and bulk-derived $4f$ final-state multiplets. The bulk lines could be represented by Doniach-Sunjić line shapes,¹⁴ convoluted by a Gaussian spectrometer function, while the surface components could be better described by pure Gaussians. These findings together with the much larger width of the surface peaks suggest that there are several overlapping surface signals due to different coordinations of surface atoms. Such effects have previously been found in a PE study of Yb metal films deposited on a substrate at liquid-He temperatures.¹⁵ In order to account for electron-electron scattering of photoelectrons on their way through the sample, an integral background (dashed curves in Figs. 1–4) was also taken into account.

The BIS spectra were analyzed in an analogous way using the known $4f$ -multiplet splittings.^{16,17} In this case the surface components were found to be negligible due to the low surface sensitivity of BIS at electron kinetic energies around 1500 eV.

III. EXPERIMENTAL RESULTS

In Fig. 1, $4f$ and $5p_{3/2}$ core-level PE spectra of Lu metal and LuAl_2 taken at a photon energy of $h\nu=70$ eV are presented; Fig. 2 shows corresponding spectra for Yb metal and YbZn_2 . The $4f$ PE spectra are dominated by emission from the $4f^{14}$ states of Lu and divalent Yb, giving rise to a superposition of bulk- and surface-derived $4f^{13}$ final-state spin-orbit-split doublets. Within the limits of

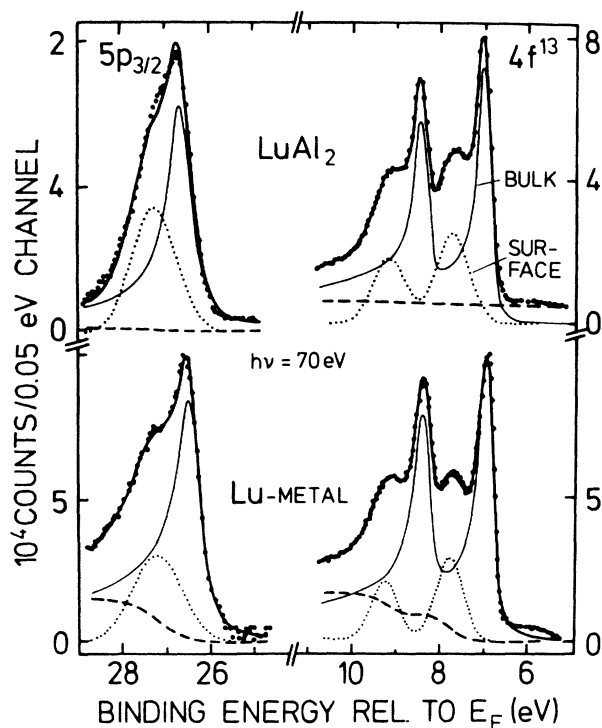


FIG. 1. $4f$ and $5p_{3/2}$ core-level PE spectra of Lu metal and LuAl_2 . The heavy solid line represents the result of a least-squares-fit analysis of the data with a superposition of two $4f^{13}$ ($5p_{3/2}$) final-state multiplets originating from the bulk (light solid curve) and the surface (dotted curve), respectively. The dashed line represents the integral background.

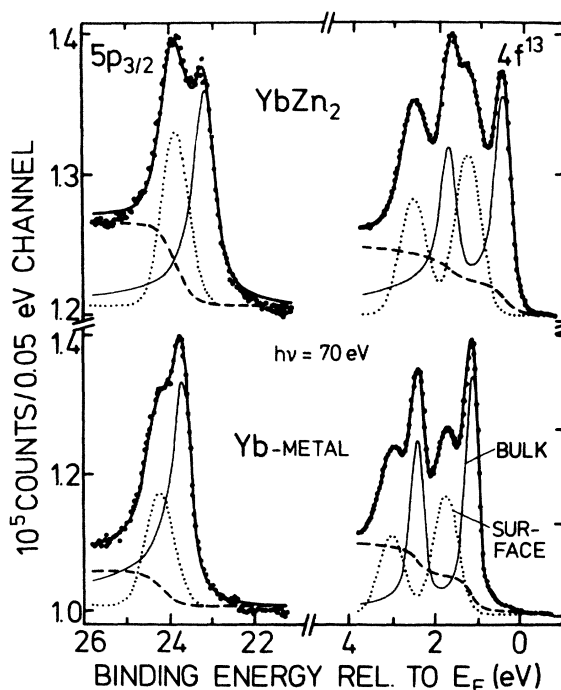


FIG. 2. $4f$ and $5p_{3/2}$ core-level PE spectra of Yb metal and YbZn_2 including the results of the least-squares-fit analysis. The $4f^{13}$ and $5p_{3/2}$ subspectra from the bulk (surface) are indicated by the light solid (dotted) curves.

the present accuracy, the observed surface shifts are identical for the $4f$ and $5p_{3/2}$ levels. A comparison of the spectra observed for the intermetallic compounds with those for the pure metals reveals distinct differences between the divalent (Yb) and trivalent (Lu) systems: While trivalent Lu in LuAl_2 shows nearly no change as compared to the pure metal, divalent Yb in YbZn_2 exhibits larger bulk and surface core-level shifts as well as a strong increase of the surface emission intensity. An analogous

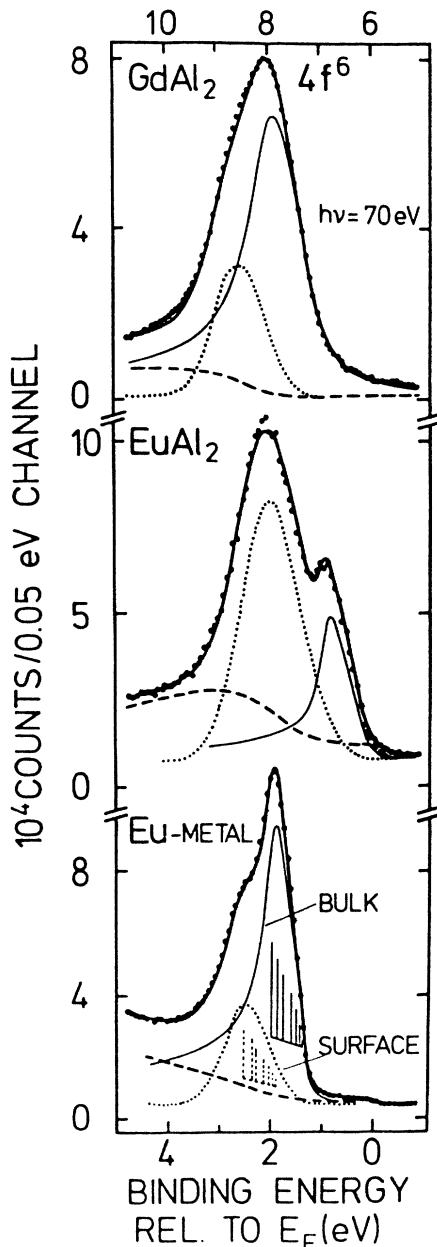


FIG. 3. $4f$ PE spectra of Eu metal, EuAl_2 , and GdAl_2 . The data were least-squares-fitted by a superposition of two $4f^6$ final-state multiplets. Positions and relative intensities of the bulk (surface) $4f^6$ multiplet are represented by the solid (dotted) bar diagram for Eu metal. Bulk (surface) contributions are indicated by the light solid (dotted) curves. Note the difference in energy zero for Eu and EuAl_2 (lower axis) and GdAl_2 (upper axis).

TABLE I. $4f$ binding energies E and chemical shifts ΔE of bulk (index B) and surface (index S) components for several RE compounds. Always the multiplet component with the lowest binding energy is used. Note that the chemical shift is defined by $\Delta E = E^{\text{met}} - E^{\text{com}}$. With the exception of Eu, Yb, and Lu, the given values for the pure metals are taken from Refs. 16 and 35; data for EuPd , EuPd_3 , and EuPd_2Si_2 were taken from Ref. 22.

Compound	E_B (eV)	E_S (eV)	ΔE_B (eV)	ΔE_S (eV)
EuAl_2	0.45	1.80	1.00	0.30
GdAl_2	7.35	8.15	0.20	-0.10
TbAl_2	2.10	2.85	0.10	-0.05
DyAl_2	3.75	4.50	0.15	-0.05
TmAl_2	4.45	5.20	0.10	0.05
YbAl_2	0.10	1.05	1.00	0.70
YbZn_2	0.50	1.35	0.60	0.40
LuAl_2	6.75	7.75	0.20	0.05
EuPd_2Si_2	0.20	1.20	1.25	0.85
EuPd	0.60	1.50	0.85	0.60
EuPd_2	0.55	1.40	0.85	0.70

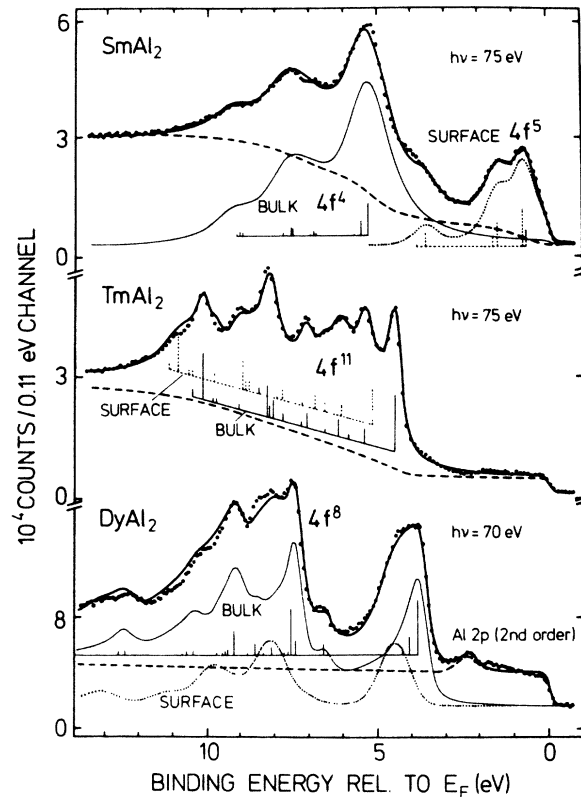


FIG. 4. $4f$ PE spectra of SmAl_2 , TmAl_2 , and DyAl_2 . The SmAl_2 spectrum was fitted by a superposition of a $4f^5$ multiplet close to E_F and a deeper-lying $4f^4$ multiplet from bulk-trivalent Sm ions. The TmAl_2 and DyAl_2 spectra were least-squares-analyzed with a superposition of two $4f^{11}$ and two $4f^8$ final-state multiplets, respectively. Positions and relative intensities of the bulk (surface) multiplets are represented by the solid (dotted) bar diagrams.

behavior of divalent and trivalent RE ions in the respective dialuminides is observed for EuAl_2 (divalent) and GdAl_2 (trivalent); relevant $4f$ PE spectra of such systems are displayed in Fig. 3. Both substances show the same $4f^6$ final state; the spectrum of divalent EuAl_2 , in contrast to that of trivalent GdAl_2 , is quite different from the one observed for pure metals. The results of the line-shape analysis concerning the positions of the bulk and surface line as well as the respective shifts relative to the pure metals are summarized in Table I.

Valence-band PE spectra of the trivalent RE compounds SmAl_2 , TmAl_2 , and DyAl_2 , taken at the indicated photon energies, are displayed in Fig. 4. The spectrum observed for SmAl_2 contains both $4f^4$ and $4f^5$ final-state multiplets, separated by the Coulomb correlation energy $U \approx 4.5$ eV. By varying the photon energy, the $4f^5$ emission near the Fermi edge, originating from divalent Sm atoms, is clearly identified as a surface feature, while the $4f^4$ final-state multiplet at higher binding energy represents the expected signal from bulk trivalent Sm atoms. This clearly shows the existence of a surface-induced valence transition in SmAl_2 , quite similar to the case of Sm metal.³ Consequently, the spectrum of SmAl_2 is well described by a superposition of a $4f^5$ multiplet

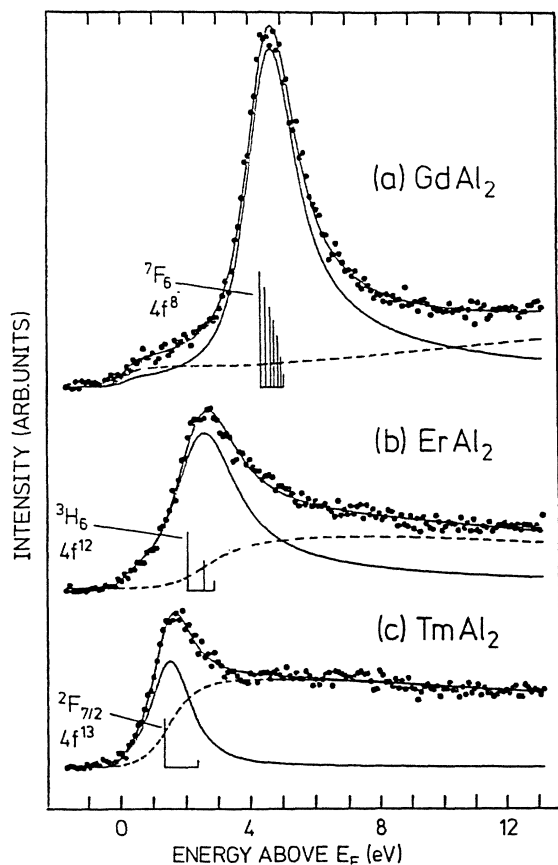


FIG. 5. BIS spectra of GdAl_2 , ErAl_2 , and TmAl_2 , taken at 1486.6 eV photon energy. The spectra were fitted using the corresponding final-state multiplets (bar diagrams and light solid curves) superimposed on an integral scattering background (dashed line). Note the lack of surface contributions due to the large mean free path of the electrons at this energy.

close to E_F and a deeper-lying $4f^4$ final-state multiplet from bulk-trivalent Sm ions. A homogeneously mixed-valent surface can be excluded from the 0.6-eV binding energy observed for the weakest bound $4f^5$ -multiplet component. Moreover, only the outermost surface layer of SmAl_2 is involved in the valence transition to the divalent state, since no surface core-level shift is found for either the $4f^5$ or the $4f^4$ final states. Thus, a complete surface valence transition is encountered in SmAl_2 ; this conclusion is in agreement with much less detailed $3d$ core-level x-ray-photoemission-spectroscopy (XPS) results.¹⁸ On the other hand, no indications for surface-induced valence changes were observed in the cases of TmAl_2 , DyAl_2 (Fig. 4), and TbAl_2 (not shown here). The $4f$ -dominated valence-band spectrum of TmAl_2 is consequently well described by a superposition of two rigidly shifted $4f^{11}$ final-state multiplets,¹⁶ accounting for electron emission from bulk and surface atoms, respectively (see Table I). This is true also for DyAl_2 , where the observed $4f$ -emission features could be reasonably well analyzed by a superposition of two rigidly shifted $4f^8$ final-state multiplets,¹⁶ which originate from bulk and surface Dy atoms.

Figure 5 shows the BIS results for GdAl_2 , ErAl_2 , and TmAl_2 . The spectra are dominated by the $4f$ final-state multiplets, since the $4f$ cross sections are much higher than the $5d$ ones. The bar diagrams in Fig. 5 represent the positions of the multiplets as derived from least-squares-fit procedures. The good quality of the fits provides no hint to surface contributions to the experimental spectra, a fact that may actually be expected from the large mean free path of electrons with a kinetic energy around 1500 eV.

The experimental results may be summarized as follows: (i) The binding-energy shifts (chemical shifts) of the bulk core levels relative to the pure metals are distinctly larger in divalent systems than in trivalent RE compounds. (ii) The surface core-level positions exhibit the same overall trend, however, with smaller shifts. (iii) In divalent compounds, the intensity of the surface component is markedly higher than in trivalent compounds. (iv) A surface valence transition from a bulk trivalent to a surface divalent state of the Sm atom is observed for SmAl_2 . (v) No surface features are identified in the BIS spectra.

IV. DISCUSSION

A. Binding energies and $4f$ -configurational stability

The $4f$ photoexcitation of a divalent ($4f^n$) RE ion leads to a trivalent ($4f^{n-1}$) final state. On the other hand, the population of an initially unoccupied $4f$ state of a trivalent RE ion in a BIS experiment results in a divalent RE impurity in the solid. If we denote the energy difference between the divalent and trivalent state by $\Delta E_{\text{II,III}}$, the binding energy E_B of the lowest level of the final-state $4f$ multiplet can be written as¹⁹

$$E_B = \Delta E_{\text{II,III}} + E_{\text{imp}}^{3+} \quad (\text{photoemission}),$$

$$E_B = \Delta E_{\text{II,III}} - E_{\text{imp}}^{2+} \quad (\text{BIS}),$$
(1)

where E_{imp} describes the heat of solution of the final-state impurity ion in the lattice, and further relaxation effects are neglected. Note that binding energies are taken as positive values for photoemission and as negative values for BIS experiments. Following Johansson,¹⁹ $\Delta E_{\text{II,III}}$ can be expressed in terms of the difference in cohesive energies of ideal divalent and trivalent RE elements plus the atomic $4f^n \rightarrow 4f^{n-1}5d$ promotional energy:

$$\Delta E_{\text{II,III}} = E_{\text{coh}}^{2+} - E_{\text{coh}}^{3+} + E(4f^n \rightarrow 4f^{n-1}). \quad (2)$$

Due to the lower coordination at the surface, the cohesive energy for a surface atom is reduced to $\approx 80\%$ of the bulk value,²⁰ leading to a corresponding shift in the core-level binding energy [surface core-level shift (SCS)].^{4,8}

In intermetallic compounds, the cohesive energies are increased by the heat of formation $-\Delta H$.^{9,10,21}

$$E_{\text{coh}}^{\text{com}} = E_{\text{coh}}^{\text{met}} - \Delta H. \quad (3)$$

Combining Eqs. (1)–(3), the chemical shift ΔE of the 4f level in a compound as compared to the elemental metal is given by

$$\Delta E = E_B^{\text{com}} - E_B^{\text{met}} = (\Delta H^{3+} - \Delta H^{2+}) - E_{\text{imp}}^{3+, \text{met}} + E_{\text{imp}}^{3+, \text{com}}. \quad (4)$$

Here, ΔH^{2+} (ΔH^{3+}) denotes the heat of formation of the divalent (trivalent) compound, and E_{imp} describes the impurity term. Trivalent RE compounds, which become tetravalent in the PE final state, may be treated in an analogous way: In this case, ΔH^{2+} and ΔH^{3+} have to be replaced by ΔH^{3+} and ΔH^{4+} , respectively, and similarly E_{imp}^{3+} by E_{imp}^{4+} .

Figure 6 displays the observed surface versus bulk chemical shifts for a number of rare-earth compounds. The approximately linear relationship between surface and bulk shifts²² directly reflects the decrease in cohesive energy at the surface. The data can be described by a straight line with a slope of about 0.7, which is slightly smaller

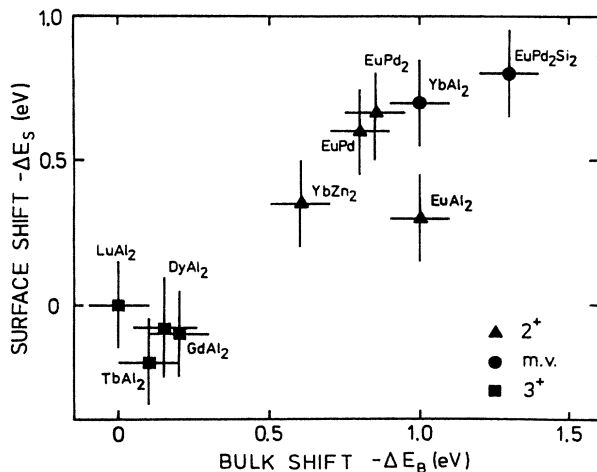


FIG. 6. Relation between the chemical shifts in 4f binding energy in the bulk and at the surface for various RE compounds. Note that $\Delta E = E^{\text{com}} - E^{\text{met}}$. m.v. denotes the mixed-valent compound.

than the one of 0.8 proposed by Johansson for RE metals.⁷ The striking result in this diagram is the separation of the data into two clearly distinct regions. On the left-hand side the trivalent RE compounds with small shifts are located, while on the right-hand side the divalent and mixed-valent compounds with larger shifts are found.

A qualitative understanding of the behavior is obtained by examining Eq. (4). The first term denotes the difference in the heat of formation between initial and final state, which may be estimated on the basis of the Miedema scheme.^{9,10} For divalent and trivalent RE ions, a value of ≈ -1 eV is obtained.²³ For a trivalent RE initial state, the corresponding difference between trivalent and tetravalent RE ions in the final state is calculated to be $\approx +0.5$ eV; in this case, the RE ion in the tetravalent final state is represented by Hf.^{9,10} The remarkable change in sign reflects the fact that a trivalent RE configuration yields the most stable chemical bond in the compounds considered here. The second term, $E_{\text{imp}}^{3+, \text{met}}$, denotes the heat of solution of a trivalent RE ion in a divalent matrix, which may also be calculated with Miedema's scheme. In case of trivalent RE metals, the second term would read as $E_{\text{imp}}^{4+, \text{met}}$, representing the heat of solution of a tetravalent RE ion in a trivalent matrix. By extrapolating Miedema's formula to infinite dilution,¹⁰ a value of ≈ 0.5 eV is obtained in both cases.¹⁹

The third term describes the heat of solution of a molecule with a trivalent (tetravalent) ion in the matrix of molecules of divalent (trivalent) RE ions. This term is difficult to estimate. We argue, however, that it is generally small. This assumption is justified by the following two arguments: (i) In general, a good solubility of similar compounds, e.g., of EuAl_2 and LaAl_2 ,⁴ with different valences of the RE ions, is observed. This indicates that despite a positive size-mismatch energy the heats of solution are negative due to an increase in entropy. Since entropy terms in intermetallic compounds are, in general, considered to be small,⁹ the resulting impurity term should be even smaller. (ii) As will be seen below, the good agreement between thermochemical data and measured 4f binding energies in PE and BIS implies that $E_{\text{imp}}^{2+, \text{com}} + E_{\text{imp}}^{3+, \text{com}} \approx 0$. Since both impurity terms are negative, however, we may follow that $E_{\text{imp}}^{2+, \text{com}} \approx E_{\text{imp}}^{3+, \text{com}} \approx 0$. Neglecting the last term in Eq. (4), we obtain for the chemical shift of the 4f level between a RE metal and a RE compound, $\Delta E = -1 - 0.5 \text{ eV} = -1.5 \text{ eV}$ for a divalent RE ion and $\Delta E = 0.5 - 0.5 \text{ eV} = 0.0 \text{ eV}$ for a trivalent RE ion, in good agreement with experiment.

The position of the divalent 4f multiplet is closely related to the stability of the divalent ground state. A divalent RE ion will become trivalent, if the gain in cohesive energy compensates the 4f promotional energy. On the other hand, for a trivalent RE metal, any decrease in cohesive energy, caused by reduction of the coordination at the surface, may lead to a transition to a divalent state (surface valence transition). For elemental RE metals, Johansson derived the stability scheme shown in the left-hand part of Fig. 7.⁴ In this diagram the open circles denote the divalent-to-trivalent transition energies for bulk metals. Since we will use this diagram in connection

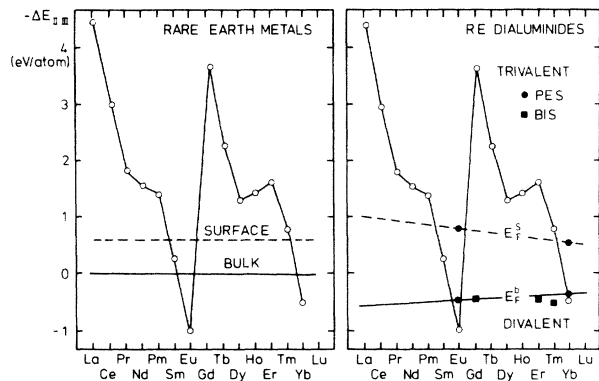


FIG. 7. Energy difference $\Delta E_{II,III}$ between the divalent and trivalent configurations of RE metals (theory) and RE dialuminides (experiment). Horizontal lines denote the relative position of the Fermi level in the bulk and at the surface, respectively. In the case of the RE dialuminides, these lines are extrapolated from measured $4f$ binding energies from PE (solid circles) and BIS (solid squares) measurements. Open circles represent the position of the Fermi edge relative to the $4f$ level; circles below the horizontal lines denote a stable divalent configuration.

with spectroscopic data, we denote the line of zero as the Fermi level E_F^B . In the case of zero impurity energy in Eq. (4) the points in the diagram correspond to $4f$ positions as measured for divalent RE metals with PE and for trivalent RE metals with BIS. The difference in relative stabilities of the RE configurations at the surface leads to a shift of the whole curve. In Fig. 7 we have instead represented this shift by a different line of zero denoted by E_F^S . The data points below the lines of zero indicate stable divalent ground-state configurations. Consequently, Eu and Yb metal are divalent in the bulk, whereas Sm metal exhibits a divalent configuration only at the surface. According to Eq. (3), the formation of an intermetallic compound adds the heat of formation to the cohesive energy of the pure metal, which can be represented by a shift of the Fermi level in the stability diagram. This shift can be directly inferred from the measured $4f$ energy positions in the PE and BIS spectra. Neglecting the impurity terms as discussed above, the measured binding energies are, according to Eq. (1), identical to the $\Delta E_{II,III}$ stability energies of the Johansson scheme.²⁴ Since the data points in this diagram represent the lowest final-state multiplet terms, the new position of the Fermi level for the compounds can be plotted easily using the measured $4f$ binding energies.

This procedure is applied to the RE dialuminides as shown in Fig. 7(b), using the PE data for divalent EuAl_2 and mixed-valent YbAl_2 ,⁶ as well as the corresponding BIS data for trivalent GdAl_2 , ErAl_2 , and TmAl_2 . The good agreement between PE- and BIS-derived Fermi levels for the bulk justifies the neglect of the impurity term *a posteriori*. The inclination of the straight lines through the bulk and surface Fermi-level data points hints to different dependences of the bulk and surface cohesive energies on the ionic radii. Of particular interest is the position and slope of the Fermi level at the surface, which for TmAl_2 predicts a stable trivalent configuration at the sur-

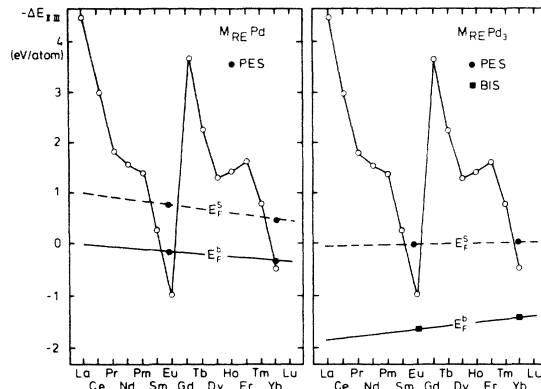


FIG. 8. Energy difference $\Delta E_{II,III}$ between divalent and trivalent configurations for the $M_{RE}\text{-Pd}$ and $M_{RE}\text{-Pd}_3$ series of compounds. Horizontal lines denote the relative position of the Fermi level in the bulk and at the surface, respectively, as extrapolated from measured $4f$ binding energies (solid circles). Open circles below the lines represent stable divalent configurations.

face [in contrast to TmS (Refs. 13 and 24)] and for SmAl_2 a surface valence transition. These predictions are in excellent agreement with observation; for SmAl_2 , even the magnitude of the measured binding energy is correctly predicted. Thus, this simple scheme allows a prediction of $4f$ configurational stability in a whole series of RE compounds, if just two compounds have been studied spectroscopically.

We finally present further convincing applications of such stability schemes for $M_{RE}\text{Pd}_x$ compounds where M_{RE} is one of the rare-earth metals. Suitable PE and BIS data are available for Eu- and Yb-based compounds.^{12,22,25} Figure 8 shows the constructed stability diagrams for the $M_{RE}\text{Pd}$ and $M_{RE}\text{Pd}_3$ series of intermetallics. The most interesting features in the context of the present discussion are the positions of the Sm- and Tm-based compounds in this diagram. The Tm compounds are found to exhibit a trivalent surface in both systems. The same holds for Sm in SmPd_3 , while for Sm in SmPd a surface valence transition is predicted, with a $4f$ binding energy of ≈ 0.4 eV. No $3d^9 4f^6$ final-state feature has been observed in the core-level x-ray PE spectrum of SmPd_3 ,²⁶ indicating the pure trivalent character of the surface layer, in perfect agreement with the present model. The case of SmPd_3 represents an illustrative example against the naive assumption that the Sm ions are generally divalent at the surface of bulk trivalent intermetallic Sm compounds.

B. Intensity of surface emission

In general, an increase in the relative weight of the intensity of surface emission in a compound as compared to the pure metal can be caused by two effects: (i) a change in the stoichiometric composition of the surface region of a solid, i.e., surface segregation; (ii) a decrease of the mean free path of the emitted photoelectrons.

In fact, surface-segregation effects have been observed

in several alloy systems.²⁷ Conceptually, the decomposition probability of a dilute binary alloy at the surface can be expressed in terms of three energy terms, namely the difference in surface energy of the pure constituents, the elastic size-mismatch energy and the heat of solution in the liquid phase.²⁷ From these three energies, the difference in surface energy is often the most important term leading to a surface enrichment of the constituent element with the lower surface energy. In the case of the systems studied here, and substituting the surface energies for divalent and trivalent RE ions by the ones for Sr and Y, values of about 430 and 1100 mJ/m² are obtained, respectively, while for Al and Zn surface energies of 1200 and 1020 mJ/m² have been calculated.²⁸ Therefore, from these surface energy considerations, segregation effects may be expected in the case of divalent compounds, whereas trivalent compounds should be rather stable. Values for the heat of solution, calculated within Miedema's scheme,¹⁰ are only half as large for the divalent case than for the trivalent compounds. Furthermore, the large molar volume of the divalent RE ions (≈ 34 cm³/mol) as compared to trivalent ones (≈ 20 cm³/mol) and particularly to Al (≈ 10 cm³/mol) leads to a much higher size-mismatch energy in the divalent systems, so that surface segregation is favored in this class of compounds. However, Miedema's scheme is strictly applicable only to the case of dilute alloys. For ordered compounds, the energy loss due to size mismatch has to be replaced by the gain in lattice energy, which in the case of close-packed Laves phases may be high enough to stabilize the bulk composition of the compound at the surface.

Considering the RE compounds studied here, the smaller than expected chemical shift observed for EuAl₂ (see Fig. 6) could be a consequence of an Eu enrichment at the surface. However, YbZn₂ and YbAl₂, which show the same high intensity ratio of surface-to-bulk emission, are in good agreement with the general correlation between bulk and surface shifts. Moreover, the quantitative agreement between the constructed stability diagrams and the experimental observations, especially for SmAl₂ (see Fig. 7), seem to contradict a model based on surface segregation.

It is interesting to compare these considerations with the results of thin-film-deposition experiments with Yb and Sm on Al single-crystal surfaces.^{29,30} For divalent Yb, strong interdiffusion effects were found even at room temperature, leading to the formation of YbAl₂ and YbAl₃ when the substrate was heated, and finally to a complete dissolution of the Yb ions in the bulk lattice. A monolayer of divalent Yb ions, however, remains stable at the surface in all cases. For Sm, no diffusion effects were reported. Disordered monolayers of Sm deposited on an Al(001) surface exhibit a mixed-valent behavior, and may be transformed to an ordered trivalent overstructure by heat treatment. The findings for the Yb-Al system are in good agreement with expectations based on Miedema's scheme, and support the concept of possible segregation effects in divalent RE compounds. However, the observation that no compound formation takes place in the Sm-Al system and the fact that the heat-treated Sm

monolayer on Al(001) is trivalent (in contrast to SmAl₂) demonstrate the differences between intermetallic compounds and adsorbate-substrate systems in the present context.

Discussing surface segregation in intermetallic RE compounds, a PE study of Yb-Au alloys is of special interest.³¹ The disordered alloys were produced by evaporating thin Au films on a substrate of polycrystalline Yb metal. Strong interdiffusion effects were found leading to the appearance of separate bulk and surface signals in the valence-band PE spectra from the divalent Yb ions. The surface-to-bulk intensity ratio of the Yb 4f subpeaks reflected a strong increase with decreasing Yb concentration in the bulk, which was explained by enhanced surface segregation of Yb. However, this explanation is not obviously consistent with the observed 4f binding energies. Compared to Yb metal, the chemical shift of the surface component is correlated to the one of the bulk by a factor of 0.8. This correlation was found to be valid up to an Au content of about 20 at.%, whereas for higher Au concentrations, the correlation factor increases. For a stoichiometric composition at the surface, a factor of 0.7–0.8 is expected according to Johansson's model, whereas any increase of the Yb concentration at the surface should lead to a decrease of the correlation factor (since the surface composition would be closer to elemental Yb metal). On the basis of the observed chemical shifts, surface segregation of Au is therefore suggested, which is in contradiction, however, to the observation of an enhanced Yb 4f surface-to-bulk intensity ratio.

An alternative explanation of this peculiar behavior can be given by considering the mean free path λ of photoelectrons emitted from a RE compound. This quantity can be written as^{32,33}

$$\lambda = \lambda_v \lambda_c / (\lambda_v + \lambda_c), \quad (5)$$

where λ_v (λ_c) denotes the mean-free-path contribution due to scattering of the hot electrons by valence electrons (core electrons). λ_c is approximately proportional to the core-level binding energy,³⁴ and much larger than λ_v , so that its contribution to the mean free path may be neglected in most cases.³³ In divalent and homogeneously mixed-valent RE compounds, however, a localized 4f level is positioned near or immediately below E_F , and hence could strongly affect the mean free path λ_c . Applying the theory of Penn³² to Yb metal, an unreasonably small value of $\lambda_c = 0.25$ Å is obtained. This failure of the theory may be caused by the neglected reduction of the 4f scattering probability due to shielding of the 4f orbitals by the 5s and 5p states. Furthermore, the small radial extent of the 4f orbital may lead to a decrease in the scattering cross section. Further theoretical and experimental work is evidently necessary to clarify this point. Nevertheless, it should be qualitatively correct that a decrease in the 4f binding energy cause a decrease in the electron mean free path. This effect, in turn, leads to a reduction of the bulk signal and to the observed enhancement of the surface emission.

In conclusion, there are several arguments in favor of surface segregation in divalent and mixed-valent RE compounds. On the other hand, effects from changes in the

mean free path cannot be excluded when considering possible causes for the high surface-to-bulk intensity ratio in core-level PE spectra of these materials.

V. SUMMARY AND CONCLUSIONS

The dialuminides of the heavy RE metals were studied by high-resolution PE in the photon-energy range $20 \leq h\nu \leq 110$ eV and by high-energy BIS at a photon energy of 1486 eV. Surface core-level shifts were resolved in the 4*f* PE spectra of all compounds studied and, in a few cases, also for deeper-lying 5*p*_{3/2} core lines. Within experimental accuracy, the surface shifts for the two core levels were found to be identical. For a number of RE intermetallics, a linear relation between surface and bulk core-level binding-energy shifts relative to the elemental metals was observed, where the surface shifts amount to only $\approx 70\%$ of the bulk chemical shifts. This observation is shown to be due to a reduction in the cohesive energy at the surface of these compounds. Moreover, the divalent and homogeneously mixed-valent compounds exhibit much larger chemical shifts than the trivalent RE compounds. This phenomenon is caused by the high heat of formation for trivalent metallic RE compounds and can be explained qualitatively within Miedema's scheme.

With the measured PE and BIS 4*f* energies, stability diagrams for the divalent and trivalent RE configurations were constructed. In agreement with the stability diagram

for $M_{RE}Al_2$ compounds, a divalent surface layer was observed for bulk-trivalent $SmAl_2$, while $TmAl_2$ exhibits no valence change at the surface. Similarly, a trivalent surface layer is predicted for $SmPd_3$, in perfect agreement with the experimental observations. Therefore, a generalization of these results seems to be justified in the following sense: The 4*f*-configurational stability in a whole series of RE compounds may be correctly predicted from spectroscopic results for only two compounds.

For divalent and homogeneously mixed-valent compounds, a systematically higher surface-to-bulk intensity ratio was found as compared to trivalent compounds. Changes in the electron mean free path due to binding-energy-dependent 4*f* scattering as well as surface segregation of rare-earth ions were discussed as possible causes for this phenomenon.

ACKNOWLEDGMENTS

The authors gratefully acknowledge the support of D. E. Eastman, the help of R. A. Pollak and G. Hollinger, as well as the assistance of the staff of the Synchrotron Radiation Center at the University of Wisconsin—Madison. T. Penney generously provided the $EuAl_2$ single crystal studied and R. D. Parks the $LuAl_2$ sample. This work was supported by the Deutsche Bundesministerium für Forschung und Technologie, Projekt Nr. 05-241 KA.

*Present address: Institut de Physique, Université de Neuchâtel, CH-2000 Neuchâtel, Switzerland.

¹P. H. Citrin, G. K. Wertheim, and Y. Baer, *Phys. Rev. Lett.* **44**, 1425 (1978).

²J. F. van der Veen, F. J. Himpsel, and D. E. Eastman, *Phys. Rev. Lett.* **44**, 189 (1980).

³G. K. Wertheim and G. Creelius, *Phys. Rev. Lett.* **40**, 813 (1978).

⁴B. Johansson, *Phys. Rev. B* **19**, 6615 (1979).

⁵W.-D. Schneider and C. Laubschat, *Phys. Rev. B* **20**, 4416 (1979).

⁶G. Kaindl, B. Reihl, D. E. Eastman, R. A. Pollak, N. Mårtensson, B. Barbara, T. Penney, and T. S. Plaskett, *Solid State Commun.* **41**, 157 (1982), and references therein.

⁷G. Kaindl, W.-D. Schneider, C. Laubschat, B. Reihl, and N. Mårtensson, *Surf. Sci.* **126**, 105 (1983).

⁸B. Johansson and N. Mårtensson, *Phys. Rev. B* **21**, 4427 (1980).

⁹A. R. Miedema, R. Boom, and F. R. de Boer, *J. Less-Common Met.* **41**, 283 (1975).

¹⁰A. R. Miedema, *J. Less-Common Met.* **46**, 67 (1976).

¹¹D. E. Eastman, J. J. Donelon, N. C. Hien, and F. J. Himpsel, *Nucl. Instrum. Methods* **172**, 327 (1980).

¹²C. Laubschat, G. Kaindl, E. V. Sampathkumaran, and W.-D. Schneider, *Solid State Commun.* **49**, 339 (1984); C. Laubschat, Ph.D. thesis, Freie Universität Berlin, 1984 (unpublished).

¹³G. Kaindl, C. Laubschat, B. Reihl, R. A. Pollak, N. Mårtensson, F. Holtzberg, and D. E. Eastman, *Phys. Rev. B* **26**, 1713 (1982).

¹⁴S. Doniach and M. Šunjić, *J. Phys. C* **3**, 285 (1970).

¹⁵W.-D. Schneider, C. Laubschat, and B. Reihl, *Phys. Rev. B* **27**, 6538 (1983).

¹⁶J. K. Lang, Y. Baer, and P. A. Cox, *J. Phys. F* **11**, 121 (1981).

¹⁷P. A. Cox, *Struct. Bonding (Berlin)* **24**, 59 (1975); P. A. Cox and J. K. Lang (unpublished); W. T. Cornell, P. R. Fields, and Rajnak, *J. Chem. Phys.* **49**, 4424 (1968).

¹⁸S. Raen and R. D. Parks, *Phys. Rev. B* **27**, 6469 (1983).

¹⁹B. Johansson, *Phys. Rev. B* **20**, 1315 (1979).

²⁰A. S. Skapski, *Acta Metall.* **4**, 576 (1956).

²¹A. R. Miedema, *J. Less-Common Met.* **46**, 167 (1976).

²²V. Murgai, L. C. Gupta, R. D. Parks, N. Mårtensson, and B. Reihl, in *Valence Instabilities*, edited by P. Wachter and H. Boppard (North-Holland, Amsterdam, 1982), p. 299.

²³W. C. M. Mattens, F. R. de Boer, A. K. Niessen, and A. R. Miedema, *J. Magn. Magn. Mater.* **31-34**, 241 (1983).

²⁴N. Mårtensson, B. Reihl, A. Pollak, F. Holtzberg, and G. Kaindl, *Phys. Rev. B* **25**, 6522 (1982).

²⁵M. Domke, C. Laubschat, E. V. Sampathkumaran, M. Prietsch, T. Mandel, and G. Kaindl, *Phys. Rev. B* **32**, 8002 (1985).

²⁶F. U. Hillebrecht and J. C. Fuggle, *Phys. Rev. B* **25**, 3550 (1982).

²⁷A. R. Miedema, *Z. Metallkd.* **69**, 456 (1978).

²⁸A. R. Miedema, *Z. Metallkd.* **69**, 287 (1978).

²⁹R. Nyholm, I. Chorkendorff, and J. Schmidt-May, *Surf. Sci.* **143**, 177 (1984).

³⁰A. Fäldt and H. P. Myers, *Phys. Rev. B* **30**, 5481 (1984).

³¹L. I. Johansson, A. Flodström, S. E. Hörnström, B. Johansson, J. Barth, and F. Gerken, *Solid State Commun.* **41**, 427 (1982).

³²D. R. Penn, *J. Electron Spectrosc. Relat. Phenom.* **9**, 29 (1976).

³³J. Szajman and R. C. G. Leckey, *J. Electron Spectrosc. Relat.*

Phenom. **23**, 97 (1981).

³⁴C. J. Powell, *Surf. Sci.* **44**, 29 (1974).

³⁵F. Gerken, J. Barth, R. Kammerer, L. I. Johansson, and A. Flodström, *Surf. Sci.* **117**, 468 (1982).